Zeitschrift: Botanica Helvetica
Herausgeber: Schweizerische Botanische Gesellschaft
Band: 100 (1990)
Heft: 1

Artikel: Immunofluorescence and ultrastructure of mitosis and cell division in the fern Athyrium filix-femina

Autor: Jenni, V. / Cattelan, H. / Roos, U.-P.

DOI: https://doi.org/10.5169/seals-69714

Botanica Helvetica 100/1, 1990

0253-1453/90/010101-19 $ 1.50 + 0.20/0

Immunofluorescence and ultrastructure of mitosis and cell division in the fern *Athyrium filix-femina*

V. Jenni, H. Cattelan and U.-P. Roos

Institute of Plant Biology, University of Zürich, Zollikerstr. 107, CH-8008 Zürich, Switzerland

Manuscript accepted December 15, 1989

Abstract

Jenni V., Cattelan H. and Roos U.-P. 1990. Immunofluorescence and ultrastructure of mitosis and cell division in the fern *Athyrium filix-femina*. Bot. Helv. 100: 101–119.

We studied mitosis in apical cells of prothallia of the fern *Athyrium filix-femina* by DAPI fluorescence, immunofluorescence with an antibody against yeast tubulin, and electron microscopy. A preprophase band consisting of from 20 to 30 microtubules (MTs) was visible ultrastructurally in several cells, but it was never labelled in immunofluorescence preparations. A "cage" of microtubules surrounds the nucleus during prophase. As mitosis progresses, the extranuclear MT-fibers become more and more axially oriented and the spindle poles first appears as brightly fluorescent "caps" on opposite sides of the nucleus. The nucleolus concomitantly fades. Two distinct half-spindles with pointed poles are organized by metaphase; these consist mainly of kinetochore fibers, but MT bundles crossing from one half-spindle to the other occasionally occur. Kinetochores are ultrastructurally differentiated insertion points for spindle MTs. Polar fluorescence disappears rapidly during telophase, whereas interzonal fluorescence remains bright until well into cytokinesis. Phragmoplast vesicles possibly derive from dictyosomes and may be guided by MTs to the site of new wall formation. A post-cytokinetic layer of MTs subtends the new wall on either side of it.

Key words: Fern, *Athyrium filix-femina,* gametophyte, immunofluorescence, microtubules, mitosis, ultrastructure.

Introduction

Many antibodies against microtubule (MT) proteins, the tubulins, have become available in recent years, and their use in immunofluorescence of various types of plant cells and tissues has greatly advanced our knowledge about the three-dimensional arrangement and cyclical changes of MT complexes, notably also the formation and morphology of the mitotic spindle *in situ* (reviews: Gunning 1982, Gunning and Hardham 1982, Lloyd 1987).

The mitotic spindle in higher plants is typically anastral, but some cell types possess the potential to develop asters, which has been experimentally verified by Vannereau et al. (1972). Furthermore, Schmit et al. (1983) demonstrated that aster-like MT centers estab-

lish spindle polarity in endosperm cells. With the exception of certain algae, plant spindles are also acentriolar, a feature retained even in the bryophytes and pteridophytes that form basal bodies of flagella during the reproductive phase of their life cycle.

A unique feature of cell division in non-algal plants is the preprophase band (PPB; Pickett-Heaps and Northcote 1966). This cortical girdle of parallel MTs in premitotic cells is approximately 1–6 μm wide and consists of from 10–20 to over 150 MTs (e.g., Busby and Gunning 1980, Eleftheriou 1985, Gunning and Hardham 1982, Pickett-Heaps and Northcote 1966). The MTs are positioned near the plasmalemma as a virtual monolayer, or stacked up to ten deep (Burgess and Northcote 1967, Gunning and Hardham 1982); they may be closely packed (Cronshaw and Esau 1968), in clusters (Busby and Gunning 1980), or scattered (Galatis et al. 1984). Although the number of MTs in the two opposite profiles of cross-sectioned PPBs may be similar, asymmetry is common, and even essentially one-sided PPBs occur (Gunning et al. 1978). Double and forked PPBs have also been observed (Wick and Duniec 1983).

The PPB is not, however, ubiquitous in cells of higher plants, as it does not occur in some cultured cells and protoplasts (Fowke et al. 1974, Gorst et al. 1986, Simmonds 1986), in moss protonemata (see references in Gunning and Hardham 1982, Lloyd 1987, and Doonan et al. 1987), in hornwort sporophytes, and in microsporocytes of *Selaginella* (Brown and Lemmon 1985a, b). Hogan (1987) observed that the PPB is present in mitotic root cells, but not in meiocytes.

In fern protonemata, on the other hand, PPBs exist, as they do in two- and three-dimensional aggregates of bryophyte and pteridophyte cells (Brown and Lemmon 1984, Burgess 1970, Doonan et al. 1987, Fowke and Pickett-Heaps 1978, Apostolakos and Galatis 1985, Gunning and Hardham 1982, Schnepf 1984).

The exact function of the PPB remains an issue of some conjecture. It may orient the nucleus prior to mitosis (e.g., Burgess and Northcote 1967) or steer vesicles containing wall precursors to localized regions of wall synthesis (Packard and Stack 1976). The correlation between the presence of a PPB and morphogenetic order has also raised the possibility that it is a marker of tissue organization (Gunning 1982, Lindenmayer 1984, Lloyd 1987, Simmonds 1986). Gunning and collaborators (Gunning 1982, Gunning and Hardham 1982, Gunning and Wick 1985, Gunning et al. 1978) have put forth the hypothesis that the position of the PPB predicts the site where the cell plate fuses with the parental cell wall during cytokinesis and they have backed it up with painstaking and elegant observations. Lloyd (1987), however, pointed out that there is no "obligatory relationship between the former PPB site and the direction of outgrowth of the phragmoplast".

As a plant cell reaches prophase, the PPB disappears or is reduced (Gunning 1982, Kubiak et al. 1986, Pickett-Heaps and Northcote 1966, Wick and Duniec 1984, Wick 1985), but it may persist until late prophase (Burgess 1969). Tubulin fluorescence concomitantly appears associated with the nucleus and increases to give rise to a "fibrous cage" with bright polar caps (Hogan 1987, Kubiak et al. 1986, Wick 1985, Wick and Duniec 1983, 1984). In some plant cells a prophase spindle develops (Kubiak et al. 1986, Wick and Duniec 1984). The mature metaphase spindle of plant cells consists of kinetochore and non-kinetochore fibers joining at a focal or broad spindle pole (De Mey et al. 1982, Hogan 1987, Kubiak et al. 1986, Vantard et al. 1985, Wick 1985). Discrete polar structures comparable to the centrosomes of higher animal cells (Brinkley 1985) or the spindle pole bodies of many protists (Heath 1986) are generally not detectable ultrastructurally, but in a few instances polar differentiations or focal points for radiating MTs have been described (Esau and Gill 1969; Fowke and Pickett-Heaps 1978, Wilson 1970).

The concept of polar MT-organizing centers (MTOC; Pickett-Heaps 1969) perhaps visible by electron microscopy only occasionally in plant cells has received support from recent immunofluorescent observations with a human auto-antiserum that reacts with centrosomes and other MTOCs in animal cells (Clayton et al. 1985, Wick 1985).

Laminar kinetochores, as in higher animals and many protists (Fuge 1977, Heath 1980) occur among the plants only in some algae (Godward 1985, Pickett-Heaps and Fowke 1969). Other localized, as opposed to diffuse kinetochores (e.g., Braselton 1981), may have the 'cup and ball' shape as in the superbly suitable, though not universally typical endosperm cells of *Haemanthus* (Bajer and Molè-Bajer 1969), or they may be visible as a whispy fuzz of lesser density than the chromosomes (e.g., Fowke et al. 1974). Consequently, the ends of kinetochore MTs (kMTs) are not precisely lined up and they can often not be exactly determined.

After the disintegration of the nuclear envelope (NE), remnants of its membranes commonly occur at the spindle periphery, often delimiting the spindle body against the surrounding cytoplasm (review: Hepler and Wolniak 1984). In addition to polar caps of endoplasmic reticulum (ER), an elaborate system of membrane cisternae has also been revealed *in* the spindle, notably in association with kinetochores (Schmiedel et al. 1981). As calcium has been co-localized with such membranes (Wick and Hepler 1980, Wolniak et al. 1980), they may be involved in the regulation of MT assembly and disassembly by sequestering or releasing Ca^{2+} (Hepler and Wolniak 1984).

Microtubules in plant spindles are not strictly aligned along the spindle axis or towards the spindle poles. Oblique or slanted MTs are found among both the kMTs and the non-kinetochore MTs (nkMTs) (e.g., Bajer 1973, Jensen 1982). Whether such arrays are the structural correlates of chromosome movements via interactions between MTs (Bajer 1973, Fuge et al. 1985) remains debatable.

Cell plate formation during cytokinesis also involves MTs (Esau and Gill 1969, Gunning 1982, Hepler and Jackson 1968). As bundles of MTs join to form the phragmoplast, they may direct or move vesicles that carry cell plate precursors to the sites of wall polymer synthesis (Hepler and Jackson 1968, Gunning 1982).

In higher cryptogams, nuclear and cell division has been incompletely documented, although descriptive ultrastructural aspects are published for members of all the classes (Brown and Lemmon 1982a, b, c, 1984, 1985a, b, 1988, Burgess 1970, Busby and Gunning 1980, Fowke and Pickett-Heaps 1978, Lambert 1977, Manton 1964, Schmiedel et al. 1981, Schnepf 1984). Whereas immunofluorescence has been successfully applied to MTs of mosses (Doonan et al. 1985, 1987), no fern has been studied with this technique. One reason is that tissues which are otherwise very suitable, as root tips of *Azolla,* have so far proved refractory to the use of tubulin antibodies (Wick 1985).

In an attempt to fill gaps in our knowledge of mitosis in the pteridophytes we investigated nuclear and cell division in the fern *Athyrium filix-femina* by combining tubulin immunofluorescence and transmission electron microscopy. Prothallia are very suitable objects for such a purpose, as they are easy to grow the year round and the apical notch and lateral lobes, where mitoses are quite frequent, are but a single cell layer thick. Using an antibody raised against yeast tubulin (Kilmartin et al. 1982), which is specific for the tyrosinated form of the α-monomer (Wehland et al. 1984), and employing MT-stabilizing conditions during fixation (Schroeder et al. 1985) we succeeded in revealing cytoplasmic and spindle MTs by immunofluorescence. The PPB, however, was only detectable in ultrathin sections. In many respects mitosis in *A. filix-femina* is very similar to that of other cormophytes, but it also exhibits features unique for very few cryptogams.

Materials and methods

Organism and growth conditions

Prothallia were grown in Petri dishes from spores collected by Dr. J. Schneller in the Lake Zurich area. Some spores were sown onto agar made 2% in Mohr's (1956) nutrient solution. Alternatively, spores were sieved through eight layers of lens cleaning tissue to separate the remains of sporangia. Samples of these spores were either sown directly onto Knop's nutrient agar [1.0 g $Ca(NO_3)_2$, 0.25 g KCl, 0.25 g $MgSO_4$, 0.25 g KH_2PO_4, 1% agar, per 1000 ml distilled water; a few drops of a sterile 2 mM solution of $FeCl_3$ were added after autoclaving] and swelled in the dark for 24 h (Dyer 1979), or they were first surface-sterilized (modified from Dyer 1983). To this end the spores were wetted with 0.4% Teepol or 0.5% Triton X-100 (Merck) in water, pelletted in a table-top centrifuge, resuspended in distilled water and swelled for 24 h in the dark (Dyer 1979). After another centrifugation the spores were treated for 40 sec with an aqueous solution of 0.7% sodium hypochlorite (NaOCl), recentrifuged, washed in sterile distilled water, and plated on the surface of Knop's agar. A well was cut in the center of each agar layer for periodic watering with nutrient solution or sterile distilled water.

The culture plates were placed at room temperature in ambient light conditions or exposed to the light of a fluorescent tube (Osram L White, 40 W) that provided a photoperiod of 12 h from 7 AM to 7 PM. Prothallia were used after 6–9 weeks of culture.

Coverslip preparations for light microscopy

Prior to each fixation for immunofluorescence or electron microscopy, sample prothallia were stained for 1 h with an aqueous solution of 1 μg/ml DAPI (Lin et al. 1977) containing 0.2% Triton X-100 and examined with a fluorescence microscope for the presence of mitotic figures. When this preliminary test was positive, prothallia were fixed for electron microscopy, or attached to coverslips lightly coated with diluted Rubber Cement, immediately covered with MSB, and processed for immunofluorescence.

Immunofluorescence

The methods of Doonan et al. (1983), Simmonds et al. (1985) and modifications thereof were tried in vain. A modified version of the method used by Schroeder et al. (1985) eventually led to success. All the steps described hereafter were carried out in a moistened Petri dish. The buffer over the prothallia was replaced for 10 min with a solution of 10% DMSO in MSB. This solution was drawn off and the prothallia were fixed for 1 h with 3.7% formaldehyde (prepared fresh from *p*-formaldehyde) in MSB containing 10% DMSO. After three rinses with MSB the material was treated for 1 h for the partial digestion of cell walls. The solution employed was a mixture of the following enzymes in 0.1 M PIPES, pH 5.9, and 3 mM EGTA: 2% cellulase (Sigma), 2% cellulysin (Calbiochem), 1% driselase (Fluka), 2% hemicellulase (Sigma), 2% macerocyme R-10 (Serva), 2% pectinase (Sigma), 2% pectolyase (Sigma), 1% bovine serum albumin (Fluka), 1 mM PMSF, 0.1% PVP, and 0.2 M D-mannitol.

Following digestion the preparations were rinsed with MSB, permeabilized for 30 min with MSB containing 2% Triton X-100 and 10% DMSO, and rinsed again in MSB and TBS. Normal goat serum (Nordic) was applied at 5% in TBS for 60 min, after which the prothallia were rinsed and incubated overnight with the monoclonal antibody YL 1/2 of Kilmartin et al. (1982). After several rinses with TBS, FITC-labelled goat anti-rat IgGs (Nordic) were applied for 2 h. The preparations were rinsed again with TBS, stained with a solution of 1 μg DAPI/ml TBS for 10 min, rinsed once more with TBS and embedded in 90% glycerol containing the fading retardant *p*-phenylenediamine (Johnson and de Nogueira Araujo 1981).

Light microscopy

A Zeiss Photomicroscope III was used for phase contrast microscopy, and a Photomicroscope II equipped with a III RS epifluorescence condensor, an HBO 50 W mercury arc lamp, and the

appropriate filters (cf. Roos et al. 1986) was used for fluorescence microscopy. Phase contrast micrographs were taken on Kodak Technical Pan 2415 film and fluorescence micrographs on Kodak Plus-X-Pan. Development was in HC-110, dilution 1 + 39 for 8 min, or dilution 1 + 15 for 5½ min, respectively, at 20 °C.

Electron microscopy

Small blocks of agar with prothallia were cut from the culture dishes and transferred to pill glasses containing Karnovsky's fixative (1965; straight, or modified according to Millonig 1976). A drop of diluted Triton X-100 was sometimes added to improve wetting of the prothallia. The vessels were evacuated until all the samples were submerged. Fixation was for 2 h at room temperature. The prothallia were rinsed with three changes of 20 min each in 0.06 M or 0.2 M Na-phosphate buffer, pH 7.2, at 5 °C, after which a postfixation with 1% osmium tetroxide in the same buffer followed for 2 h or over night at 5 °C. Prothallia were rinsed in two changes of cold buffer and once with distilled water at room temperature. Staining *en bloc* was with 2% aqueous uranyl acetate for ½ or 2 h at room temperature or at 60 °C (Locke et al. 1971). The prothallia were freed of the agar during the subsequent washing step in water. They were dehydrated in ethanol and embeded in the epoxy resin of Spurr (1969) in plastic molds or according to the sandwich technique (Reymond and Pickett-Heaps 1983). The notch region of selected prothallia was cut out and glued to a resin stub. Semithin sections were cut on a Reichert Om-U3 or Ultracut microtome with glass knives and transferred to a drop of water on a slide, which was dried on a hot plate. A drop of immersion oil was applied, the sections were covered with a coverslip and examined with phase contrast optics. When mitotic cells were located, the block was retrimmed and ultrathin sections were cut with a diamond knife. Sections were picked up on copper grids (50-mesh or single hole) coated with formvar and carbon and post-stained with 2% aqueous uranyl acetate for 20 min, followed by lead citrate for 2 min. Sections were examined with a Hitachi HU-11E or H-7000 electron microscope at 50 or 75 kV.

Abbreviations used

DAPI = 4′-6-Diamidino-2-phenylindol × 2 H_2O (Serva); DMSO = dimethylsulfoxide (Serva); EDTA = ethylenediaminetetraacetic acid (Fluka); EGTA = ethylene glycol-bis(β-amino-ethyl ether)N,N,N′,N′-tetraacetic acid (Serva); MES = 2-(N-morpholino)ethanesulfonic acid (Serva); MSB = MT-stabilizing buffer: 50 mM MES, pH 6.7, 50 mM KCl, 2 mM $MgCl_2$, 10 mM EGTA, 1 mM EDTA; PIPES = piperazine-N,N′-bis(2-ethanesulfonic acid) (Calbiochem); PMSF = phenylmethylsulfonyl fluoride (Fluka); PVP = polyvinylpyrrolidone (Serva); Tris = tris(hydroxymethyl)-aminomethane (Fluka); TBS = Tris-buffered saline.

Results

Immunofluorescence of MTs during the mitotic cycle

Because the prothallia were not squashed, they retained their considerable thickness. Micrographs therefore represent optical sections in different planes of the spindle. We found no preprophase band in any of the 106 prothallia examined. Prometaphase and anaphase stages, which are certainly the shortest ones in the mitotic cycle, were also absent.

In early prophase the chromosomes were slightly condensed and the nucleolus was visible (Figs. 1 a, c). Microtubules were present just outside the nucleus, with a defined orientation in grazing optical sections (Fig. 1 a). In para-median optical sections of the nucleus the cage of MTs appeared as a fluorescent ring (Fig. 1 b), with some fibers extending into the cytoplasm. In later stages of prophase, the spindle poles became

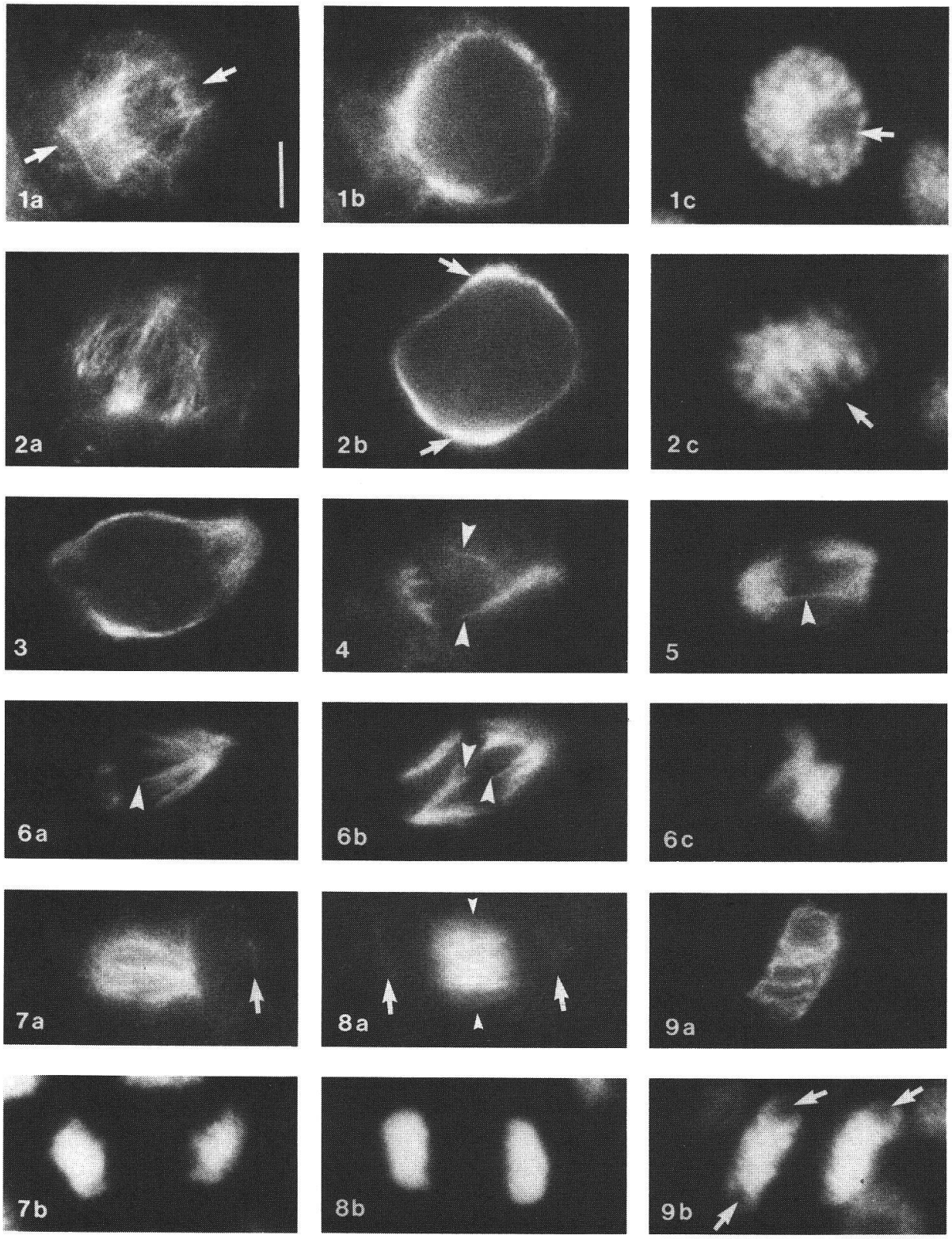
1a
1b
1c
2a
2b
2c
3
4
5
6a
6b
6c
7a
8a
9a
7b
8b
9b

Figs. 1–9. Tubulin immunofluorescence and DAPI staining patterns.

Fig. 1. Early prophase. a Optical section just above the nucleus. Tubulin fluorescence suggests a fibrous cage around the nucleus, with an indication of predominant orientation of the fibers along a defined axis (arrows). b Median optical section of the same nucleus, which is surrounded by a fluorescent ring from which some fibers run into the cytoplasm. c DAPI pattern: the chromosomes are slightly condensed; a nucleolus appear as a darker area (arrow) inside the nucleus. Bar = 5 μm.

Fig. 2. Mid-prophase. a The axial orientation of fluorescent fibers is more distinct than in Fig. 1 a. b The brighter fluorescence in the presumptive pole areas (arrows) is striking in this median optical section of the nucleus. c DAPI pattern: chromosome condensation is advanced; the arrow points to a nucleolar remnant.

Fig. 3. Mid- to late prophase. The right-hand pole is clearly a defined area where fluorescence is intense and where fibers run together. The left-hand pole (out of focus in this plane) was very similar.

Fig. 4. Late prophase. The poles of the nascent spindle are pointed; fluorescent fibers run along and over the nucleus (arrowheads).

Fig. 5. Metaphase. Tubulin fluorescence is concentrated in the two half-spindles, which are connected by a fiber (arrowhead).

Fig. 6. Metaphase. a, b Half-spindles are distinctly tapered towards the poles; kinetochore fibers (arrowheads) end near the spindle equator. c DAPI-stained chromosomes aligned at the spindle equator, arms trailing in the direction of the spindle axis.

Fig. 7. Telophase. a One forming daughter nucleus is partly surrounded by a dot pattern (arrow). Fluorescent fibers, oriented axially, are prominent in the interzone. b DAPI-staining: the chromosomes are still recognizable in the forming daughter nuclei.

Fig. 8. Late telophase. a The nascent phragmoplast (arrowheads) is discernible as a darker band across the bright interzonal fibers. Weak fluorescence remains at the poles (arrows). b DAPI-staining: the chromosome are partially decondensed.

Fig. 9. Cytokinesis. a Only phragmoplast MTs remain between the daughter nuclei. b DAPI-stained daughter nuclei with reforming nucleoli (arrows).

visible, first as broad focal regions, later as distinct bundling points of the spindle fibers (Figs. 2–4). Short bundles of MTs extended from the poles to the nuclear envelope and along it; other fibers were running over the surface of the nucleus (Fig. 4).

In metaphase the chromosomes were assembled at the spindle equator, their arms preferentially oriented along the spindle axis (Fig. 6c). Microtubule fluorescence was brightest near the poles, fanning out towards the spindle equator as several fibers, most of which ended at the chromosomes (Figs. 5, 6a and b). Occasionally, MT bundles extended from one half-spindle to the other (Fig. 5).

Telophase chromosomes were individually visible during early stages, but decondensed during later stages (Figs. 7–9). The nucleolus was again present in late telophase/cytokinesis (Fig. 9b). The MT pattern varied much between early and late telophase (Figs. 7a–9a). Fluorescence was weak or absent at the poles, presumably because the MTs were disassembled. Microtubule density, as judged by the intensity of fluorescence, was greatest in the interzone between the daughter nuclei. Fluorescence was diffuse at the periphery of the interzonal spindle remnant, but deeper inside short fibers running parallel to the former spindle axis were distinct (Figs. 7a, 8a). A perpendicular nonfluorescent line represented the phragmoplast (Fig. 8a).

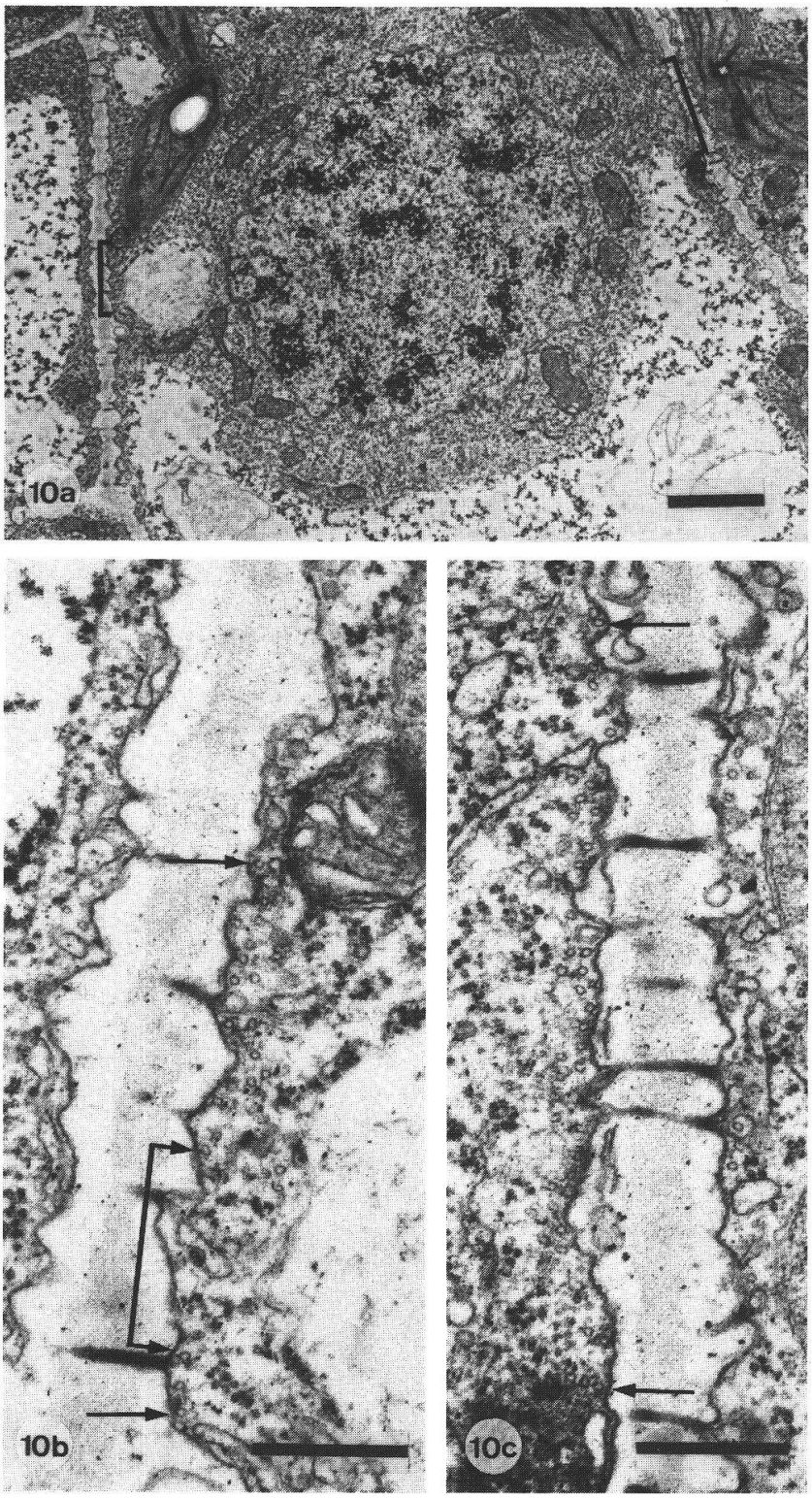

Fig. 10. a Partial overview of a cell in preprophase. The brackets mark the location of the cross-sectioned MTs of the PPB. Bar = 2 μm. b, c The bracketed parts of a at higher magnification; the arrows mark the width of the PPB profiles. Note that the profile in b has a gap (arrowed bracket) and that it consists only of 18 MTs, whereas 31 MTs compose the opposite profile shown in c. Bar = 0.4 μm.

Ultrastructural observations

Except perhaps for the occasionally slightly more condensed chromatin (Fig. 10a) there is no gross feature that distinguishes preprophase cells from other interphases in ultrathin sections. The detection of preprophase was therefore the result of a painstaking examination of a large number of cells in search of a cortical band of cross-sectioned MTs in a plane that transsects the nucleus (Figs. 10b and c). We counted as many as 31 MTs per PPB profile, but the numbers differed by as much as 13 on opposite sides of a cell (Figs. 10b and c). Some PPBs were split into two subgroups of MTs (Fig. 10b). Generally, the MTs were close to the cell membrane, but occasionally a few were several nm removed or stacked towards the cell interior (Figs. 10b and c). In the vicinity of the nuclear surface of early preprophase cells a few short MT profiles without a defined orientation were visible. At a later stage (Fig. 11), when the higher degree of chromosome condensation compared to interphase indicated the transition to prophase, there were numerous obliquely sectioned MTs around the nucleus, which, although short, were clearly oriented towards two opposite focal areas lying on an axis perpendicular to the plane of the PPB. The compact PPB consisted of 18 MTs on one side and of 20 MTs on the opposite side of the cell (Fig. 11).

In early prometaphase (Fig. 12), long fragments of the nuclear envelope (NE), some in intimate association with individual chromosomes, partially still delimited the nucleoplasm from the cytoplasm (Figs. 12b–d). MTs were more numerous in the cytoplasmic than in the nucleoplasmic area, but most converged towards the spindle pole areas (Fig. 12c). Short, unoriented MT profiles and cross-sections of MTs occurred at both poles (Fig. 12c), as did a few double membranes of ER, mitochondria, and a dictyosome.

Fig. 11. Composite of MT tracings from six consecutive serial sections of a pre-prophase cell. The cell wall is stippled and the quasi-circular outlines represent chloroplasts and mitochondria. Short lines represent the numerous obliquely sectioned MTs that surround the nucleus (N). The solid outline of the nucleus is from the first, the stippled outline is from the last section of the series. The profiles of the PPB (arrows) are symbolically marked – there were 18 MTs in the profile on the left and 20 MTs in the profile on the right. Bar = 2 μm.

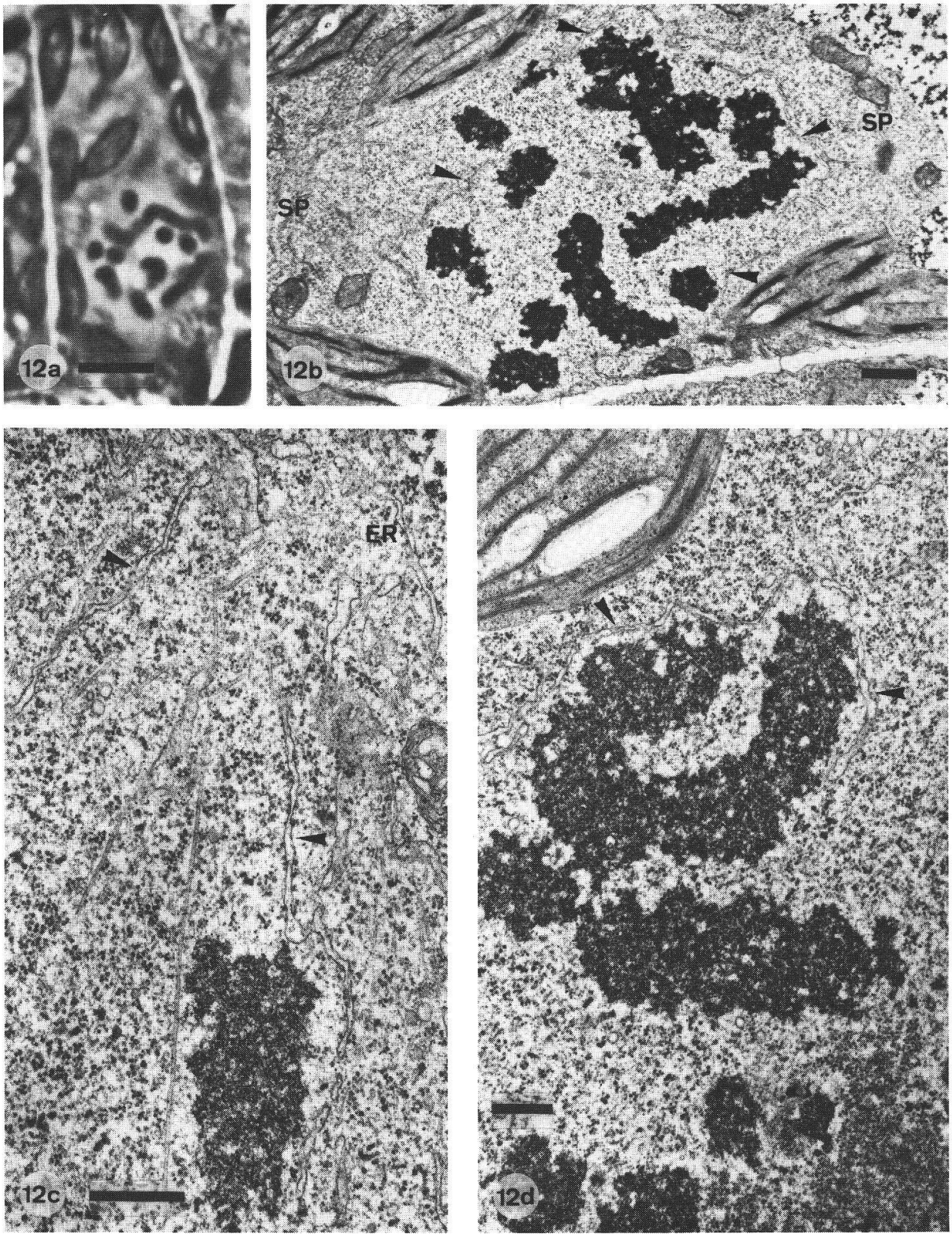

Fig. 12. Prometaphase. a Phase contrast micrograph of a semithin section of the cell shown in b to d. Bar = 2 μm. b Survey electron micrograph (rotated by ca. 90° relative to a, c), showing the areas of the spindle poles (SP) and large fragments of the nuclear envelope (arrowheads). Organelles, such as mitochondria and chloroplasts are excluded from the spindle region, but a dictyosome is situated at the right-hand pole. Bar = 1 μm. c The area of the left spindle pole shown in b at higher magnification in a serial section. Fragments of the NE (arrowheads) mingle with cisternae of the endoplasmic reticulum (ER); MTs run along chromosomes towards the pole area, where other MT profiles are oriented in different directions. Bar = 0.5 μm. d Detail of the periphery of the chromosome group, partially wrapped by large fragments of the NE (arrowheads). Part of the nucleolus is visible in the lower right corner. Bar = 0.5 μm.

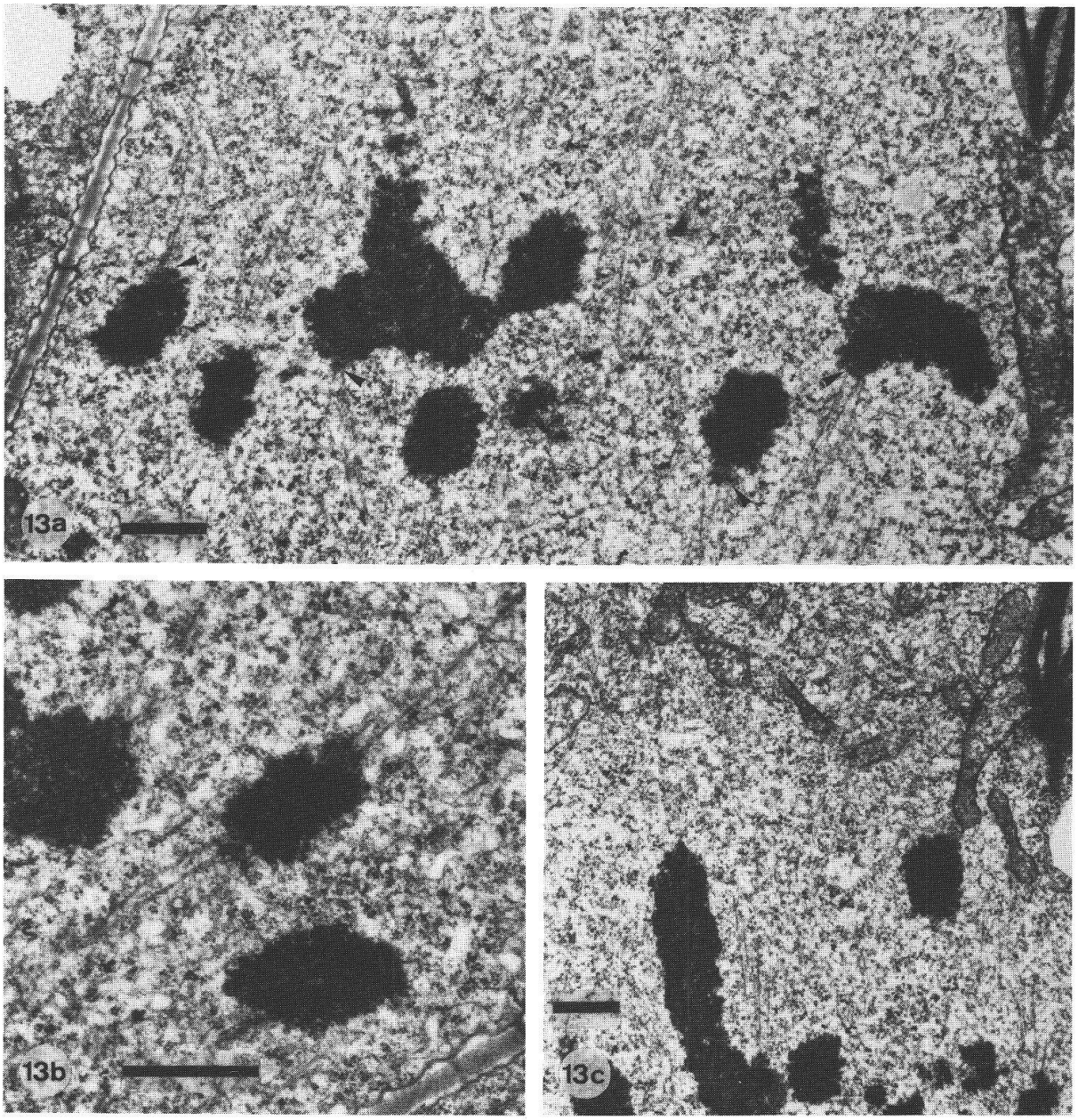

Fig. 13. Metaphase. a Overview of the chromosomes aligned at the spindle equator. Kinetochores (arrowheads) are visible on several of them. Bar = 1 μm. b Detail of a chromosome with sister-kinetochores oriented towards opposite poles. Bar = 1 μm. c Overview of the pole region. Long chromosome arms are oriented along the spindle axis, as are most MTs. Organelles have not invaded the spindle area. Bar = 1 μm.

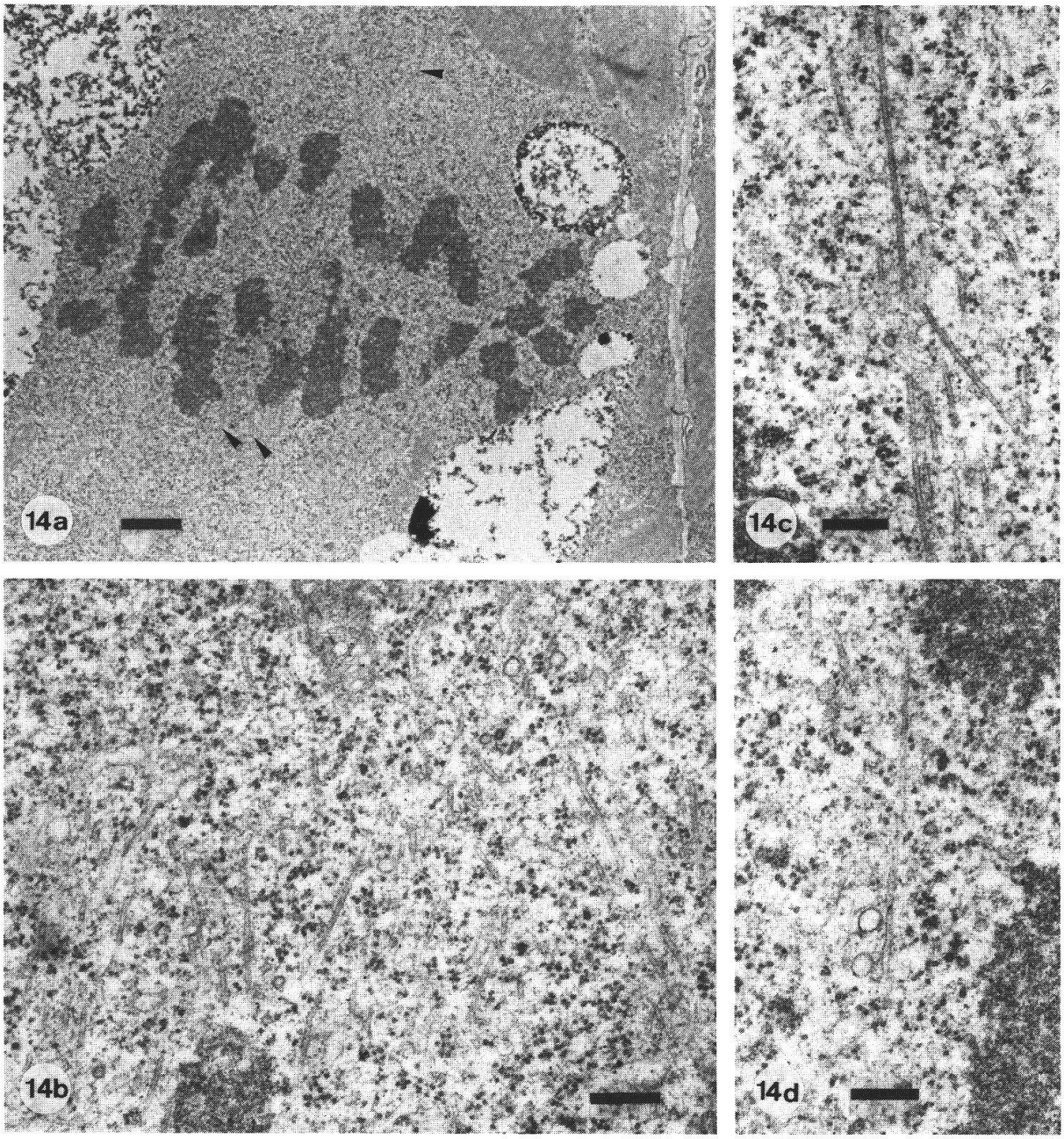

Fig. 14. Anaphase. a Overview showing the two groups of chromosomes and bundles of MTs poleward of these (arrowheads). Bar = 1 μm. b Detail of the area poleward of the chromosomes (from a section serial to a). The MTs slant at various angles and in various directions, but none lies clearly across the spindle. Bar = 1 μm. c MTs of a kinetochore bundle belonging to a chromosome just off the lower edge of the picture. Note the parallel and slanting MTs. Bar = 1 μm. d Detail from the interzone; two spherical vesicles lie close to an MT that runs parallel ot the spindle axis. Bar = 1 μm.

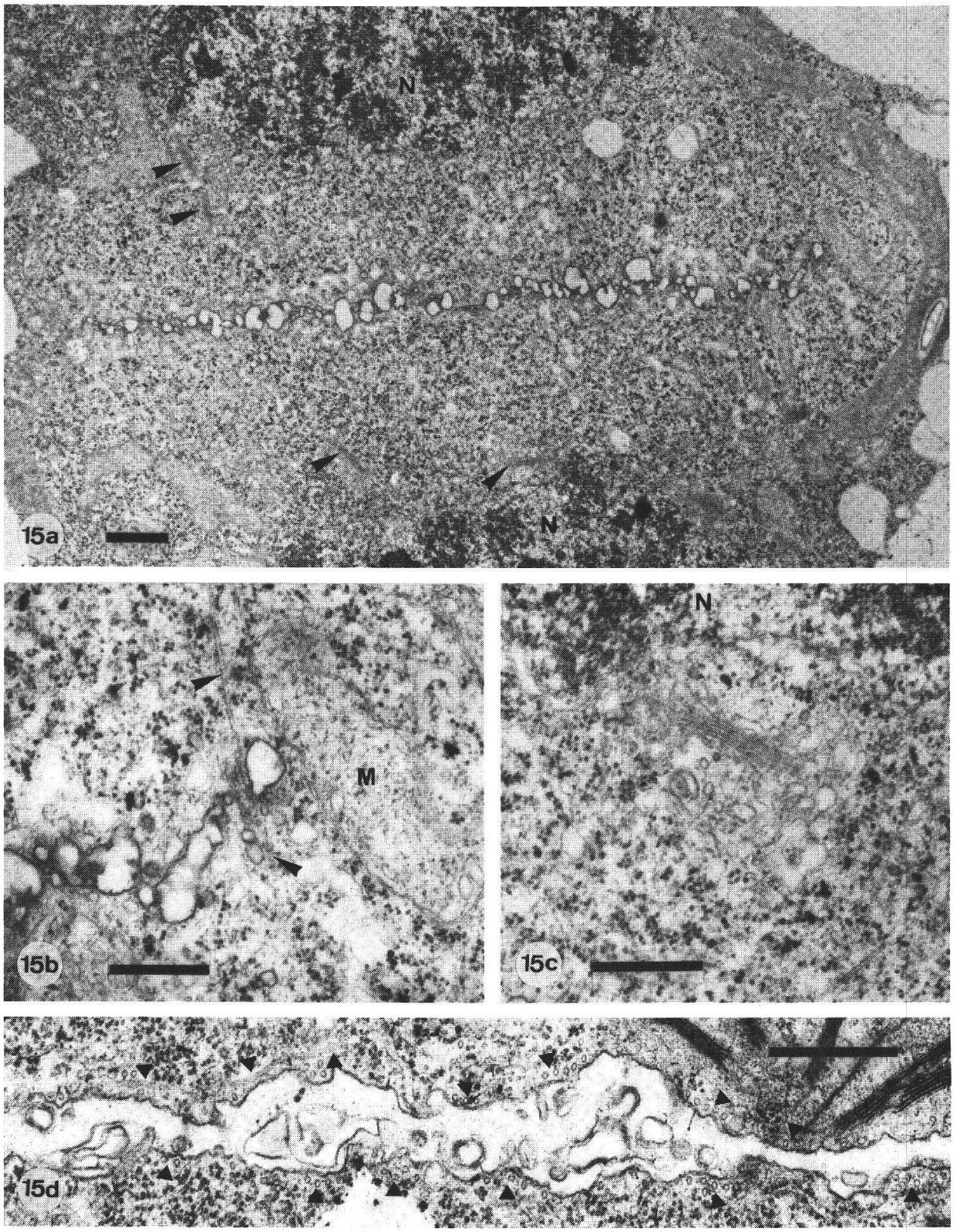

Fig. 15. Telophase – early cytokinesis (a to c) and postcytokinesis (d). a Overview showing the interzonal faces of the two daughter nuclei (N) and the phragmoplast. Dictyosomes occur close to the daughter nuclei (arrowheads). Bar = 1 μm. b Detail from the right edge of the phragmoplast shown in a. The phragmoplast vesicles are bordered on the right by a mitochondrion (M). MTs run between two larger vesicles (arrowheads). Bar = 0.5 μm. c Interzonal face of a daughter nucleus (N) with a large dictyosome (from a section serial to a). Bar = 0.5 μm. d Cell plate between two post-cytokinetic daughter cells. Note the many cross-sectioned MTs and the two obliquely cut ones near the left margin (arrowheads). Bar = 0.5 μm.

The nucleolus, still visible, had a loosely granular texture (Fig. 12d). No trace of a PPB was detectable at this stage and no kinetochores were recognizable.

At metaphase (Fig. 13), the kinetochore areas of the chromosomes were more or less aligned at the spindle equator, but the chromosome arms, especially the long ones, extended in the spindle axis a considerable distance towards the spindle poles (Fig. 13c). Bundles of MTs were axially oriented with little convergence towards the pole areas. Kinetochores appeared as fibrous, non-laminar structures set off from the chromatin by a less dense layer (Fig. 13b). Dictyosomes, ER, and mitochondria were excluded from the spindle body (Figs. 13a, c).

Anaphase (Fig. 14) was characterized by numerous MT profiles poleward of the daughter chromosomes. Although generally oriented towards the spindle pole areas, many of them slanted at a considerable angle in various directions (Fig. 14b). Bundles of kMTs were also often traversed by slanting MTs (Fig. 14c). In the interzone, where spherical vesicles occurred here and there, MTs were less numerous (Fig. 14d).

In early telophase the daughter chromosomes were aggregated, but still recognizable as discrete units, at opposite sides of the cell. Membrane fragments, ER, and MTs occurred deep between the chromosomes. Many MTs could also be found along the interzonal face of the forming daughter nuclei. In mid-telophase the phragmoplast consisted of numerous vesicles that were larger in the center than at the periphery (Fig. 15a). Long MT profiles were prevalent in the interzone between the phragmoplast and the chromosomes; they seemed to terminate among vesicles (Fig. 15b). Mitochondria were typically associated with the edges of the phragmoplast (Fig. 15b), but also with the poleward faces of the daughter nuclei, and large dictyosomes occurred near the interzonal face of the daughter nuclei (Figs. 15a, c). In late stages of telophase the chromosomes were decondensed to form a single mass of heterochromatic and euchromatic patches. The NE closely followed the contours of this mass and the nucleolus was ultimately visible again. Chromosome decondensation and the re-formation of the NE were completed before the vesicles of the phragmoplast had coalesced to form the cell plate.

In several serial sections of two adjacent cells we found a row of cross-sectioned MTs on either side of the cell wall (Fig. 15d), but also a few oblique profiles. We searched carefully for the opposite complement of MT cross-sections in each of the two cells, but found none. We were therefore not observing two PPBs in adjacent cells, but a post-cytokinetic double layer of MTs oriented parallel to the newly formed cell wall.

Discussion

The formation of the mitotic spindle and its breakdown in prothallia of *A. filix-femina* are preceded, accompanied, and followed by changes in the MT pattern, a phenomenon observed in most plant cells that have been investigated by indirect immunofluorescence. This species of fern can now also be added to the growing list of taxa (Gunning 1982) with a well-developed PPB. Although it was not revealed by the immunostaining, the ultrastructural evidence disperses any doubt about its existence. If such arrays of MTs were a common feature of all or most interphase cells, we should have found them very frequently in ultratrathin sections. Odds of sampling or a particular lability of PPB MTs under conditions of fixation are unsatisfactory explanations for our failure to detect the PPB by immunofluorescence, especially in view of the fact that PPBs have been revealed together with other MTs in several plant species (Doonan et al. 1987, Hogan 1987,

Kubiak et al. 1986, Wick and Duniec 1983, Wick et al. 1981). As shown by Wehland et al. (1984), YL 1/2 is an antibody specific for tyrosinated α-tubulin and it is conceivable that MTs of the PPB contained mostly or exclusively the post-translationally detyrosinated form of this monomer (cf. Gundersen et al. 1984) in contrast to other interphase MTs (data not shown) and the mitotic spindle. Microtubules containing tyrosinated tubulin are less stable and more dynamic than MTs containing detyrosinated tubulin (e.g., Kreis 1987), properties one would expect of a structure as transient as the PPB. The discrepancy between our immunofluorescence and ultrastructural results are, however, rendered enigmatic by the fact that Schroeder et al. (1985) did detect the PPB in meristematic cells of *Allium cepa* with the YL 1/2 antibody.

Beginning in late preprophase (Fig. 11) MTs appear around the nucleus in a preferred orientation approximately perpendicular to the plane of the PPB, i.e., roughly in the direction of the future spindle axis. Division polarity is thus established before the onset of prophase, but the process continues throughout this stage in the sense that the number of MTs of the perinuclear "cage" increases and their axial alignment becomes more evident in the form of fibers. The polar "caps" of MTs concomitantly appear as an additional element re-enforcing the axial polarity. This contrasts with the situation in onion root cells, where polar "caps" of tubulin fluorescence indicate polarization as early as late preprophase when the PPB is still present (Kubiak et al. 1986, Wick and Duniec 1984). The prophase array of MTs in *A. filix-femina* occupies a perinuclear area that appears as "clear zone" in differential interference contrast (Bajer and Molè-Bajer 1969).

The spatial control over polymerization of the MTs of the perinuclear "cage" has been discussed by many authors. The fact that no discrete MTOC is present led Schnepf (1984) to suggest that these MTs arise from diffuse organizing "zones". The NE itself has also been considered as having an initiating capacity for the nucleation of MTs during prophase (De Mey et al. 1982, Hogan 1987, Kubiak et al. 1986, Lambert 1977), but an electron-dense coat on the outer nuclear membrane as the possible structural correlate of an extensive MTOC has been shown only by Lambert (1977). On the other hand, MT initiation material is localized at the poles as early as prophase (Wick 1985).

We have obtained no evidence for the establishment of a prophase spindle and its dissolution at the beginning of prometaphase, as observed in onion root cells (Kubiak et al. 1986). Rather, spindle formation in *A. filix-femina* proceeds without such a hiatus. The metaphase spindle of *A. filix-femina* is quite tapered towards the poles (cf. Mineyuki et al. 1988, Schroeder et al. 1985), which is more typcial for centric spindles that have discrete focal structures at the poles (Weber and Osborn 1979). As in most other plants there are no discrete polar structures in *A. filix-femina* spindles, but exceptions to this rule have been observed, notably during meiosis in a moss (Brown and Lemmon 1982c).

The metaphase spindle clearly consists of two half-spindles that in turn are constituted mostly by kMTs, although some bundles of nkMTs traverse the spindle equator. The axial orientation of the spindle MTs forces the longer chromosome arms to extend towards one or the other of the spindle poles, like in endosperm cells *in vitro* (Bajer and Molè-Bajer 1969). Larger organelles are excluded, as is typical for animal and plant cells with open spindles (e.g., Fuge 1977, Roos 1973), but vesicles that may be part of the calcium-sequestering system for the regulation of spindle function (Hepler and Wolniak 1984) are a consistent spindle component.

The mature and oriented metaphase kinetochores are not layered, but they resemble the "ball-in-a-cup" type (Bajer and Molè-Bajer 1969) in as far as they are less electron-opaque than the chromosomes and sit in centromeric dimples. During anaphase the chromosomes move poleward on a broad front, which suggests that the poles widen

compared to metaphase. For lack of appropriate stages in the immunofluorescence preparations we could not verify this conclusion. Presumably, anaphase is very short and fast, so that in any sample of cells this stage is rare. There is a surprising degree of disorder among the MTs in front of the chromosomes during anaphase, which may be significant with regard to the mechanism of movement (Bajer 1973, Fuge et al. 1985) or simply the consequence of MT breakdown.

From the immunofluorescence preparations it is obvious that a shift in the number of MTs occurs from the spindle areas poleward of the chromosomes to the interzone during telophase. Large dictyosomes lying near the interzonal face of the daughter nuclei possibly elaborate vesicles that are transported along phragmoplast MTs to the site of cell plate formation where they coalesce (Hepler and Jackson 1968, Gunning 1982).

We were surprised by our discovery of the post-cytokinetic layers of MTs. Such an array has hitherto been described only by Schnepf (1984) in young *Sphagnum* leaflets as evidence for a further shift of MTs to another system prior to the re-formation of the subplasmalemmal interphase array. Further studies will have to critically examine the conclusion that post-cytokinetic MT layers are restricted to cryptogamic plants.

We thank Dr. J. Schneller for generous gifts of spores and much helpful advice on the culture of prothallia.

References

Apostolakos P. and Galatis B. 1985. Studies on the development of the air pores and air chambers of *Marchantia paleacea*. III. Microtubule organization in preprophase-prophase initial aperture cells – formation of incomplete preprophase microtubule bands. Protoplasma 128: 120–135.

Bajer A. S. 1973. Interaction of microtubules and the mechanism of chromosome movement (zipper hypothesis). 1. General principle. Cytobios 8: 139–160.

Bajer A. and Molè-Bajer J. 1969. Formation of spindle fibers, kinetochore orientation, and behavior of the nuclear envelope during mitosis in endosperm. Fine structural and *in vitro* studies. Chromosoma 27: 448–484.

Braselton J. P. 1981. The ultrastructure of meiotic kinetochores of *Luzula*. Chromosoma 82: 143–151.

Brinkley B. R. 1985. Microtubule organizing centers. Annu. Rev. Cell Biol. 1: 145–172.

Brown R. C. and Lemmon B. E. 1982a. Ultrastructure of meiosis in the moss *Rhynchostegium serrulatum*. I. Prophasic microtubules and spindle dynamics. Protolasma 110: 23–33.

Brown R. C. and Lemmon B. E. 1982b. Ultrastructure of sporogenesis in the moss *Amblystegium riparium*. I. Meiosis and cytokinesis. Amer. J. Bot. 69: 1096–1107.

Brown R. C. and Lemmon B. E. 1982c. Ultrastructural aspects of moss meiosis: review of nuclear and cytoplasmic events during prophase. J. Hattori Bot. Lab. 53: 29–39.

Brown R. C. and Lemmon B. E. 1984. Plastid apportionment and preprophase microtubule bands in monoplastidic root meristem cells of *Isoetes* and *Selaginella*. Protoplasma 123: 95–103.

Brown R. C. and Lemmon B. E. 1985a. Preprophasic establishment of division polarity in monoplastidic mitosis of hornworts. Protoplasma 124: 175–183.

Brown R. C. and Lemmon B. E. 1985b. A cytoskeletal system predicts division plane in meiosis of *Selaginella*. Protoplasma 127: 101–109.

Brown R. C. and Lemmon B. E. 1988. Cytokinesis occurs at boundaries of domains delimited by nuclear-based microtubules in sporocytes of *Conocephalum conicum* (Bryophyta). Cell Motil. Cytoskel. 11: 139–146.

Burgess J. 1969. Two cytoplasmic features of prophase in wheat root cells. Planta 87: 259–270.

Burgess J. 1970. Interactions between microtubules and the nuclear envelope during mitosis in a fern. Protoplasma 71: 77–89.

Burgess J. and Northcote D. H. 1967. A function of the preprophase band of microtubules in *Phleum pratense*. Planta 75: 319–326.
Busby C. H. and Gunning B. 1980. Observations on pre-prophase bands of microtubules in uniseriate hairs, stomatal complexes of sugar cane, and *Cyperus* root meristems. Eur. J. Cell Biol. 21: 214–223.
Clayton L., Black C. M. and Lloyd C. W. 1985. Microtubule nucleating sites in higher plant cells identified by an auto-antibody against pericentriolar material. J. Cell Biol. 101: 319–324.
Cronshaw J. and Esau K. 1968. Cell division in leaves of *Nicotiana*. Protoplasma 65: 1–24.
De Mey J, Lambert A.-M., Bajer A. S., Moeremans M. and De Brabander M. 1982. Visualization of microtubules in interphase and mitotic plant cells of *Haemanthus* endosperm with the immuno-gold staining method. Proc. Nat. Acad. Sci. USA 79: 1898–1902.
Doonan J. H., Cove D. J. and Lloyd C. W. 1983. Brief cellulase treatment permits anti-tubulin staining of an entire filamentous organism (moss). In: Potrykus I., Harms C. T., Hinnen A., Hütter R., King P. J. and Shillito R. D. (eds.) Protoplasts 1983, Poster Proceedings. Basel: Birkhäuser, 214–215.
Doonan J. H., Cove D. J. and Lloyd C. W. 1985. Immunofluorescence microscopy of microtubules in intact cell lineages of the moss *Physcomitrella patens*. I. Normal and CIPC-treated tip cells. J. Cell Sci. 75: 131–147.
Doonan J. H., Cove D. J., Corke F. M. K. and Lloyd C. W. 1987. Pre-prophase band of microtubules, absent from tip-growing moss filaments, arises in leafy shoots during transition to intercalary growth. Cell Motil. Cytoskel. 7: 138–153.
Dyer A. F. (ed.) 1979. The Experimental Biology of Ferns. New York: Academic Press, 657 pp.
Dyer A. F. 1983. Fern gametophytes in culture. J. Biol. Educ. 17: 23–39.
Eleftheriou E. P. 1985. Abundance of microtubules in preprophase bands of some *Triticum* species. Planta 163: 175–182.
Esau K. and Gill R. H. 1969. Structural relations between nucleus and cytoplasm during mitosis in *Nicotiana tabacum* mesophyll. Can. J. Bot. 47: 581–591.
Fowke L. C. and Pickett-Heaps J. D. 1978. Electron microscope study of vegetative cell division in two species of *Marchantia*. Can. J. Bot. 56: 457–475.
Fowke L. C., Bech-Hanse C. W., Constabel F. and Gamborg O. L. 1974. A comparative study on the ultrastructure of cultured cells and protoplasts of soybean during cell division. Protoplasma 81: 189–203.
Fuge H. 1977. Ultrastructure of the mitotic spindle. Int. Rev. Cytol. Suppl. 6: 1–58.
Fuge H., Bastmeyer M. and Steffen W. 1985. A model for chromosome movement based on lateral interaction of spindle microtubules. J. Theor. Biol. 115: 391–399.
Galatis B., Apostolakos P. and Katsaros C. 1984. Positional inconsistency between preprophase microtubule band and final cell plate arrangement during triangular subsidiary cell and atypical hair cell formation in two *Triticum* species. Can. J. Bot. 62: 343–359.
Godward M. B. E. 1985. The kinetochore. Int. Rev. Cytol. 94: 77–105.
Gorst J., Wernicke W. and Gunning B. E. S. 1986. Is the preprophase band of microtubules a marker of organization in suspension cultures? Protoplasma 134: 130–140.
Gundersen G. G., Kalnoski M. H. and Bulinski J. C. 1984. Distinct populations of microtubules: tyrosinated and non-tyrosinated α-tubulin are distributed differently *in vivo*. Cell 38: 779–789.
Gunning B. E. S. 1982. The cytokinetic apparatus: its development and spatial regulation. In: Lloyd C. W. (ed.), The Cytoskeleton in Plant Growth and Development. London, New York: Academic Press, 229–292.
Gunning B. E. S. and Hardham A. R. 1982. Microtubules. Annu. Rev. Plant Physiol. 33: 651–698.
Gunning B. E. S. and Wick S. M. 1985. Preprophase bands, phragmoplasts, and spatial control of cytokinesis. J. Cell Sci. Suppl. 2: 157–179.
Gunning B. E. S., Hardham A. R. and Hughes J. E. 1978. Preprophase bands of microtubules in all categories of formative and proliferative cell division in *Azolla* roots. Planta 143: 145–160.
Heath I. B. 1980. Variant mitoses in lower eukaryotes: indicators of the evolution of mitosis? Int. Rev. Cytol. 64: 1–80.
Heath I. B. 1986. Nuclear division: a marker for protist phylogeny? Progr. Protistol. 1: 115–162.

Hepler P. K. and Jackson W. T. 1968. Microtubules and early stages of cell-plate formation in the endosperm of *Haemanthus katherinae* Baker. J. Cell Biol. 38: 437–446.
Hepler P. K. and Wolniak S. M. 1984. Membranes in the mitotic apparatus: their structure and function. Int. Rev. Cytol. 90: 169–238.
Hogan C. J. 1987. Microtubule patterns during meiosis in two higher plant species. Protoplasma 138: 126–136.
Jensen C. G. 1982. Dynamics of spindle microtubule organization: kinetochore fiber microtubules of plant endosperm. J. Cell Biol. 92: 540–558.
Johnson G. D. and de Nogueira Araujo G. M. 1981. A simple method of reducing the fading of immunofluorescence during microscopy. J. Immunol. Meth. 43: 349–350.
Karnovsky M. J. 1965. A formaldehyde-glutaraldehyde fixative of high osmolarity for use in electron microscopy. J. Cell Biol. 27: 137A.
Kilmartin J. V., Wright B. and Milstein C. 1982. Rat monoclonal antitubulin antibodies derived by using a new nonsecreting rat cell line. J. Cell Biol. 93: 576–582.
Kreis T. E. 1987. Microtubules containing detyrosinated tubulin are less dynamic. EMBO J. 6: 2597–2606.
Kubiak J., De Brabander M., De Mey J. and Tarkowska J. A. 1986. Origin of the mitotic spindle in onion root cells. Protoplasma 130: 51–56.
Lambert A.-M. 1977. La méiose chez les Bryophytes: ultrastructure et dynamique du fuseau chez une mousse, *Mnium hornum* Hedw. Congr. Int. Bryol. 113–145.
Lin M. S., Comings D. E. and Alfi O. S. 1977. Optical studies of the interaction of 4′-6-diamidino-2-phenylindole with DNA and metaphase chromosomes. Chromosoma 60: 15–25.
Lindenmayer A. 1984. Models for plant tissue development with cell division orientation regulated by preprophase bands of microtubules. Differentiation 26: 1–10.
Locke M., Krishnan N. and McMahon J. T. 1971. A routine method for obtaining high contrast without staining sections. J. Cell Biol. 50: 540–544.
Lloyd C. W. 1987. The plant cytoskeleton: the impact of fluorescence microscopy. Annu. Rev. Plant Physiol. 38: 119–139.
Manton I. 1964. Preliminary observations on spindle fibers at mitosis and meiosis in *Equisetum*. J. Roy. Microsc. Soc. 83: 471–476.
Millonig G. 1976. Laboratory Manual of Biological Electron Microscopy. Vericelli: M. Savioto, 64 pp.
Mineyuki Y., Wick S. M. and Gunning B. E. S. 1988. Preprophase bands of microtubules and the cell cycle: kinetics and experimental uncoupling of their formation from the nuclear cycle in onion root-tip cells. Planta 174: 518–526.
Mohr H. 1956. Die Abhängigkeit des Protonemawachstums und der Protonemapolarität bei Farnen vom Licht. Planta 47: 127–158.
Packard M. J. and Stack S. M. 1976. The preprophase band: possible involvement in the formation of the cell wall. J. Cell Sci. 22: 403–411.
Pickett-Heaps J. D. 1969. The evolution of the mitotic apparatus: an attempt at comparative ultrastructural cytology in dividing plant cells. Cytobios 1: 257–280.
Pickett-Heaps J. D. and Fowke L. C. 1969. Cell division in *Oedogonium*. I. Mitosis, cytokinesis, and cell elongation. Aust. J. Biol. Sci 22: 857–894.
Pickett-Heaps J. D. and Northcote D. H. 1966. Organization of microtubules and endoplasmic reticulum during mitosis and cytokinesis in wheat meristems. J. Cell Sci. 1: 109–120.
Reymond O. L. and Pickett-Heaps J. D. 1983. A routine flat embedding method for electron microscopy of microorganisms allowing selection and precisely orientated sectioning of single cells by light microscopy. J. Microscopy 130: 79–84.
Roos U.-P. 1973. Light and electron microscopy of rat kangaroo cells in mitosis. II. Kinetochore structure and function. Chromosoma 41: 195–220.
Roos, U.-P., De Brabander M. and Nuydens R. 1986. Cell shape and organization of F-actin and microtubules in randomly moving and stationary amebae of *Dictyostelium discoideum*. Cell Motil. Cytoskel. 6: 176–185.

Schmiedel G., Reiss H.-D. and Schnepf E. 1981. Associations between membranes and microtubules during mitosis and cytokinesis in caulonema tip cells of the moss *Funaria hygrometrica*. Protoplasma 108: 173–190.

Schmit A.-C., Vantard M., De Mey J. and Lambert A.-M. 1983. Aster-like microtubule centers establish spindle polarity during interphase-mitosis transition in higher plant cells. Plant Cell Rep. 2: 285–288.

Schnepf E. 1984. Pre- and postmitotic reorientation of microtubule arrays in young *Sphagnum* leaflets: transitional stages and initiation sites. Protoplasma 120: 100–112.

Schroeder M., Wehland J. and Weber K. 1985. Immunofluorescence microscopy of microtubules in plant cells; stabilization by dimethylsulfoxide. Eur. J. Cell Biol. 38: 211–218.

Simmonds D. H. 1986. Prophase bands of microtubules occur in protoplast cultures of *Vicia hajastana* Grossh. Planta 167: 469–472.

Simmonds D. H., Seagull R. W. and Setterfield G. 1985. Evaluation of techniques for immunofluorescent staining of microtubules in cultured plant cells. J. Histochem. Cytochem. 33: 345–352.

Spurr A. R. 1969. A low-viscosity epoxy resin embedding medium for electron microscopy. J. Ultrastruct. Res. 26: 31–43.

Vannereau A., Deysson G., Benbadis M.-C., Brulfert A. and Pareyre C. 1972. Sur la formation d'asters au cours de la mitose des végétaux supérieurs. Étude ultrastructurale. C.R. Acad. Sci. (Paris) D, 275: 2477–2479.

Vantard M., Lambert A.-M., De Mey J., Picquot P. and van Eldik L. J. 1985. Characterization and immunocytochemical distribution of calmodulin in higher plant endosperm cells: localization in the mitotic apparatus. J. Cell Biol. 101: 488–499.

Weber K. and Osborn M. 1979. Intracellular display of microtubular structures revealed by indirect immunofluorescence microscopy. In: Roberts K., Hyams J. S. (eds.), Microtubules. London: Academic Press, pp. 279–313.

Wehland J., Schröder H. C. and Weber K. 1984. Amino acid sequence requirements in the epitope recognized by the tubulin-specific rat monoclonal antibody YL 1/2. EMBO J. 3: 1295–1300.

Wehland J., Schroeder M. and Weber K. 1984. Organization of microtubules in stabilized meristematic plant cells revealed by a rat monoclonal antibody reacting only with the tyrosinated form of tubulin. Cell Biol. Int. Rep. 8: 147–150.

Wick S. M. 1985. The higher plant mitotic apparatus: redistribution of microtubules, calmodulin and microtubule initiation material during its establishment. Cytobios 43: 285–294.

Wick S. M. and Duniec J. 1983. Immunofluorescence microscopy of tubulin and microtubule arrays in plant cells. I. Preprophase band development and concomitant appearance of nuclear envelope-associated tubulin. J. Cell Biol. 97: 235–243.

Wick S. M. and Duniec J. 1984. Immunofluorescence microscopy of tubulin and microtubule arrays in plant cells. II. Transition between the pre-prophase band and the mitotic spindle. Protoplasma 122: 45–55.

Wick S. M. and Hepler P. K. 1980. Localization of Ca^{++}-containing antimonate precipitates during mitosis. J. Cell Biol. 86: 500–513.

Wick S. M., Seagull R. W., Osborn M., Weber K. and Gunning B. E. S. 1981. Immunofluorescence microscopy of organized microtubule arrays in structurally stabilized meristematic plant cells. J. Cell Biol. 89: 685–690.

Wilson H. J. 1970. Endoplasmic reticulum and microtubule formation in dividing cells of higher plants – a postulate. Planta 94: 184–190.

Wolniak S. M., Hepler P. K. and Jackson W. T. 1980. Detection of the membrane-calcium distribution during mitosis in *Haemanthus* endosperm with chlorotetracycline. J. Cell Biol. 87: 23–32.